9th World Seminar on Seismic Isolation, Energy Dissipation and Active Vibration Control of Structures, Kobe, Japan, June13-16, 2005

IN-GROUND ISOLATION USING GEOSYNTHETIC LINERS

Panagiotis Georgarakos[1], Mishac K. Yegian[2], George Gazetas[1]

[1] *National Technical University, Athens, Greece*

[2] *Northeastern University, Boston, USA*

ABSTRACT

A new kind of seismic isolation is investigated: a combination of a geotextile and a high molecular weight polyethylene is inserted in the ground below the structure, to create an "isolated" soil wedge. The geosynthetic interface between the isolated and underlying soil, characterized by low and stable coefficient of friction, limits the levels of acceleration transmitted into the isolated region, even though at the expense of some relative (differential) displacements. The article investigates with finite elements the influence of the shape of this interface on the isolation effectiveness.

1. INTRODUCTION

A new concept in seismic isolation of structures has been proposed by Yegian and coworkers [2004(a,b)], who installed a low−friction interface (synthetic liner) within the foundation soil underneath the structure, instead of using seismic isolation bearings. Our goal is to develop a new inexpensive seismic isolation technology. The synthetic liner consists of a nonwoven geotextile over a suitable polyethylene. Experiments carried out by Yegian et al (2004,a) have defined the dynamic friction properties of such an interface and studied their dependence on normal stress, slippage velocity, and number of cycles. In cyclic tests the interface exhibited a static friction coefficient of 0.10 and a dynamic one of 0.07. These values proved insensitive to large variations in slippage velocity, normal stress, and number of cycles. These attributes reveal a reliable material, easy in dynamic modeling and stable under a variety of situations. More details can be found in the original papers by Yegian and coworkers.

The geometry of the low−friction interface is a key factor controlling the magnitude of the transmitted accelerations and resulting slip displacements of the "isolated" soil mass relative to the free−field. The expected significant reduction in surface acceleration is followed by slip displacements at the interface, which could perhaps result in large deformation of the isolated foundation soil and potential problems during a major earthquake.

The scope of this article is to investigate a variety of geometries of the interface. Optimal geometries of the liner are recommended, on the basis of the magnitude of the transmitted

acceleration on the overlying isolated soil mass and the ensuing slip displacements at the interface. The extent of soil deformation is also of interest in this paper.

2. SYSTEMS OF IN-GROUND ISOLATION

The geometry of the isolation liner plays a key role in the extent of the beneficial effect of the in-ground isolation. A group of five possible liner geometries are proposed and analysed in this thesis. Only 2−D plane-strain analyses are conducted, as if the interface were of infinite off-plane extent. These five in-ground isolation systems are named after the characteristic shape of the soil wedge above the liner and are presented below:

- *Cylindrical.* A simple circular geometry of the liner is analysed **[Fig.1(a)]** to develop a first understanding and a simple presentation of the system dynamics. The isolated soil wedge is a circular sector 60 m wide and 5 m deep at its middle. As this geometry might be rather difficult and expensive to achieve at the site, alternative geometries easier to construct are proposed.
- *Tub.* Here, the liner consists of a 50 m long horizontal line, 5 m deep, and two circular arcs of 5 m radius at the two edges **[Fig.1(b)].** This geometry has been proposed and already successfully tested experimentally by Yegian et al (2004,b).
- *Trapezoidal — Side angle either 30° or 60°.* The horizontal part of the liner is also 50 m long and 5 m deep, but the liner emerges at an angle of 30° (or 60°) to the horizontal **[Fig.1(c)]**. The plane surfaces are easy to construct and require less space beyond the main isolated wedge.
- *Compound Trapezoidal with reinforced core — Side angle 60°.* The liner geometry is also trapezoidal, with a side angle of 60°, but now we compact or reinforce a soil core in the middle (a truncated pyramid), where the structure will be founded **[Fig.1(d)]**. The space between the core and the non-isolated free−field soil (two inverted truncated pyramids) is backfilled with lower stiffness soil. The interface between the "reinforced" and the "loose" isolated soil is also draped with the same low friction synthetic liner. The advantages of this geometry are explored in the paper.

3. MODELING THE ISOLATED SYSTEM

Analyses are first conducted to calibrate our model against the experimental data of Yegian et al (2004,b), in terms of interface properties and observed dynamic response of the isolated soil. The experimental set-up is modeled with the finite-element code ABAQUS, and dynamic analyses at different frequencies are carried out. Parametric analysis of a full−scale system is performed under strong idealized near−fault type seismic excitation. The dimensions of the model are 360 m in width and 100 m in depth. To detect the most heavily strained areas, the soil follows an elastic−plastic Mohr−Coulomb law. The factors and parameters controlling the response are:

- the geometry of the isolation liner
- the type of soil profile. Two different 100 m deep inhomogeneous soil profiles are considered: a soft deposit **[Fig. 2(a)]** and a moderately stiff deposit **[Fig. 2(b)]**
- the soil properties of the isolated layer. The effects of Young's modulus E, friction angle φ, and cohesion c of the isolated soil are studied parametrically

- the type of seismic excitation. We use three idealized pulses (Ricker wavelets) [**Fig. 2(c)**], which can represent near-fault seismic excitations (Fardis et al 2003; Makris & Black 2004).

The dynamic motion is applied at the base of the model (100 m depth), where rigid bedrock is assumed. To define the motion at bedrock, given a desired ("control") motion at the surface, an inverse wave propagation analysis ("deconvolution") is performed with the SHAKE 91 equivalent–linear analysis program.

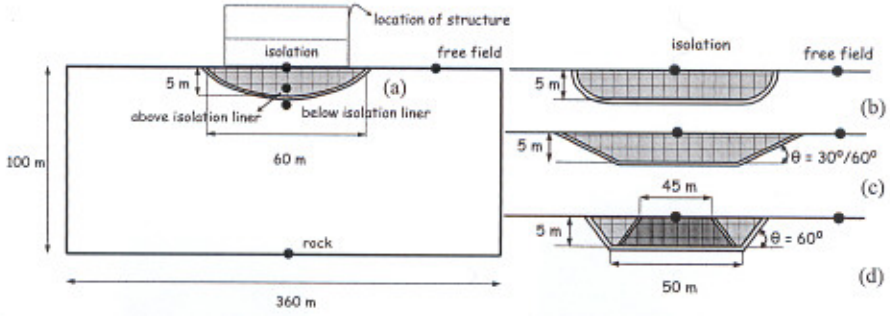

Figure 1 In-soil isolation systems: (a) cylindrical liner geometry, (b) tub liner geometry, (c) trapezoidal liner geometry, (d) compound trapezoidal liner geometry.

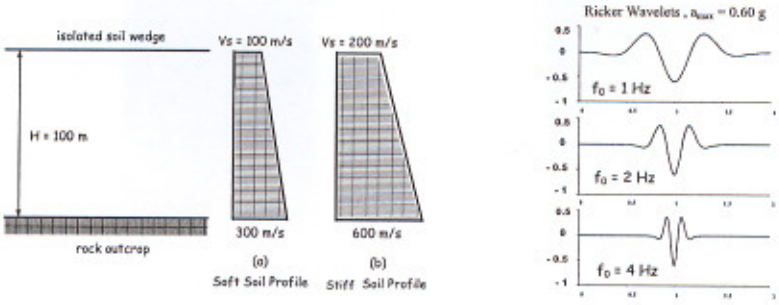

Figure 2 Shear wave velocity profiles used for the 1-D soil amplification analyses, and the idealized Ricker wavelets a(t):g with characteristic frequencies f_0 equal to 1 Hz, 4 Hz, and 4 Hz respectively.

4. RESULTS OF ANALYSIS

Calibration analyses were conducted against the experimental results of Yegian et al (2004,b). **Fig.3** presents the ratio $a_{isol,max}/a_{g,max}$ of the maximum transmitted acceleration at the center of the isolated ground surface to the peak table acceleration with respect to the latter ($a_{g,max}$), for sinusoidal table acceleration (f = 2 Hz) and Santa Cruz record from the 1989 Loma Prieta earthquake scaled to 0.6 g. We compare the experimental with the analytical results for the latter excitations.

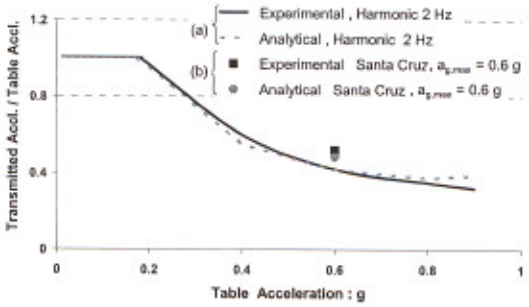

Figure 3 Comparison of experimental and analytical results for cylindrical-shaped liner : (a) harmonic excitation (frequency equal to 2 Hz), and (b) Santa Cruz record ($a_{g,max}$= 0.6 g)

4.1. Detailed Results for Cylindrical Geometry of the Liner

The first results are for the soft soil profile. Ricker wavelet of 0.66 g peak acceleration and 1 Hz characteristic frequency is the control motion. **Figs 4(a) and 5** show the acceleration and relative displacement time histories at representative nodes of the model. The following trends are worth noting:

The peak acceleration on the surface in the middle of the isolated soil wedge is equal to 0.18 g, i.e. it has decreased by a factor of 3 from the value of the "control" free–field motion. The beneficial effect of in-ground isolation is also seen in **Fig.4(b)**, which gives the response acceleration spectra at the same three nodes. The control spectrum widely exceeds the spectrum on the middle of the isolated soil. The interface sliding causes cutting-off the acceleration time histories, at the expense of slippage at the liner interface, as is illustrated in **Figs 4(a) and 5**. The maximum horizontal displacement in the middle of the isolated soil reaches 12 cm, but the residual value is substantially smaller (≈ 2 cm).

The motion of the isolated soil wedge resembles that of a rigid body, with the intra-wedge drift (the relative displacement between top and bottom of the soil wedge), barely reaches 1 cm, i.e. a 0.2% soil deformation. Therefore, soil failure is not very likely in the isolated mass.

Fig. 6 summarizes the parametric results for the free–field Ricker excitation with three characteristic frequencies (1 Hz, 2 Hz, and 4 Hz) and three peak accelerations (0.66 g, 0.44 g, and 0.22 g), for both soft and stiff soil profiles. The results are presented in terms of a_{iso}/a_{ff} ratio as a function of a_{ff} **[Fig. 6(a)]**, and of maximum slippage D_{max} at the interface, as a function of the control-motion characteristic frequency **[Fig. 6(b)]**.

Notice that the effect of in-ground isolation is insignificant when free–field acceleration, a_{ff}, has values less than 0.2 g, but that the effectiveness of isolation is an increasing function of a_{ff}. The same is also true for the spectral acceleration.

A significant reduction of the maximum slippage between the isolated soil wedge and the surrounding ground **[Fig. 6(b)]** takes place when the characteristic frequency of excitation increases, consistently with previous analytical results (Fardis et al, 2003). As expected slippage increases with increasing control acceleration. But slippage seems to be insensitive to stiffness variations in the soil profile, if the "control" seismic excitation is fixed.

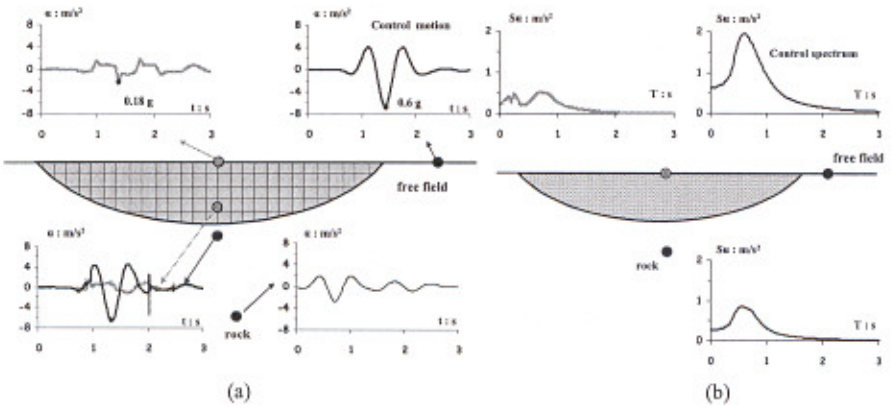

Figure 4 (a) Acceleration time histories, and (b) Response Spectral acceleration for cylindrical liner geometry. Control motion : Ricker $f_0 = 1$ Hz, $a_{ff,max} = 0.66$ g ; soft soil profile.

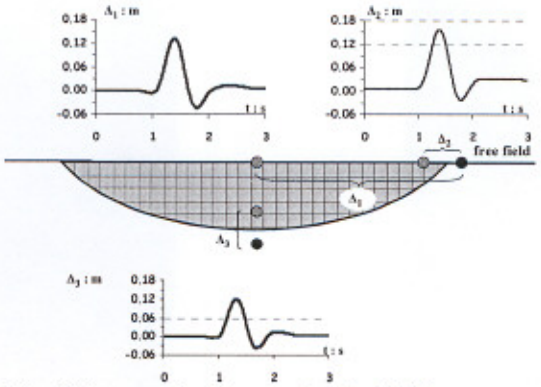

Figure 5 Relative displacement time histories for cylindrical liner geometry. Control motion : Ricker $f_0 = 1$ Hz, $a_{ff,max} = 0.66$ g ; soft soil profile.

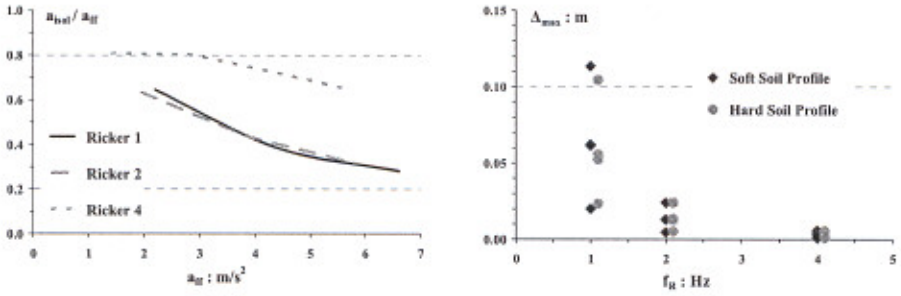

Figure 6 (a) Peak acceleration ratio (Soft soil profile), and (b) maximum slippage at the interface.

4.2 Results for the other Models

4.2.1. Tub liner geometry

Fig. 7 plots the acceleration time histories at the four representative nodes of the model (a, b, c, d). The control motion: Ricker wavelet with PGA 0.6 g and f_c = 1 Hz. The maximum acceleration developed at point "a" (the middle of the isolated soil surface) is 0.26 g, the maximum slippage is 9 cm, and the residual less than 1 cm. Compared with the cylindrical geometry: peak acceleration on the surface is higher but slippage at the liner interface is lower.

This is due to the steep ascent of the side edges, which prevent the isolated soil from sliding freely on the horizontal plane. Passive stresses develop in the adjacent free-field, which thus push the sliding wedge to return to its initial position. As greater restoring forces act in the case of the tub geometry of the liner, the acceleration values transmitted in the isolated wedge are larger, especially near the edges of the wedge (**Fig. 8**).

A side effect of the latter behavior is the development of plastic soil deformation (cracks) in both the isolated wedge and the surrounding soil. The extent of these plastic zones depends on soil strength characteristics of both the isolated and the surrounding soil. Cracking was also observed in the experiments of Yegian et al (2004,b), for the tub geometry interface. The problem could be eliminated with use of higher density isolated soil material, at the expense of increased transmitted accelerations.

4.2.2. Trapezoidal liner geometry — Side angle 30° and 60°

It is noted that as the inclination of the edges gets milder, the acceleration on the isolated soil decreases and the resulting slippage increases, as a result of the decrease of the lateral opposing thrust from the surrounding soil. The pattern of the developing plastic zones also changes.

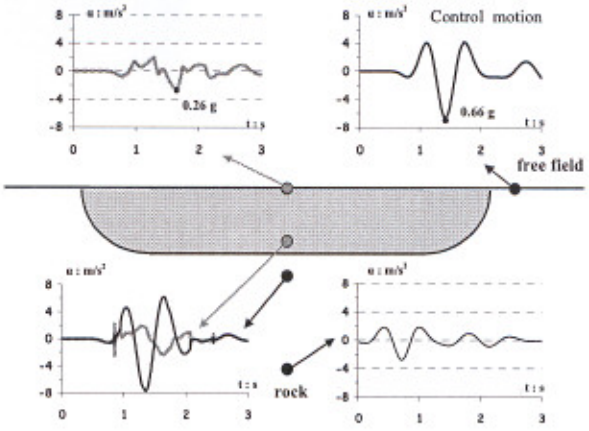

Figure 7 Acceleration time histories for tub liner geometry. Control motion : Ricker f_0 = 1 Hz, $a_{ff,max}$ = 0.66 g ; soft soil profile.

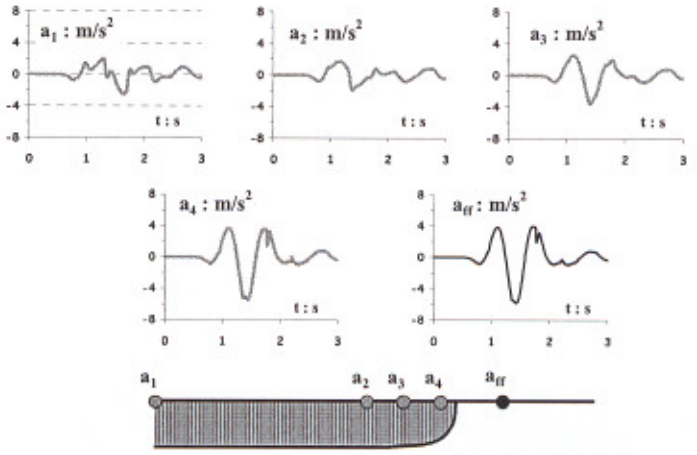

Figure 8 Acceleration time histories along the surface of the isolated soil wedge (tub liner geometry) Control motion : Ricker f_0 = 1 Hz, $a_{ff,max}$ = 0.66 g ; soft soil profile.

4.2.3. Compound Trapezoidal liner geometry — Side angle 60°

With the three previous systems a certain degree of seismic isolation is achieved, even though not as effectively as with the cylindrical liner geometry. Moreover, an area of increased plastic soil deformation is formed, which is undesirable for structures founded on the surface. For an optimal configuration which avoids these drawbacks, a composite system of in-ground isolation is proposed. The latter is a trapezoidal wedge, with compacted reinforced core and side edge angles of 60°.

Figs 9(a)–9(b) present representative acceleration and relative displacement time histories. The control motion is again a Ricker f_0 = 1 Hz wavelet with PGA = 0.6 g. The transmitted acceleration in the middle of the surface of the reinforced core does not exceed 0.2 g, whereas the maximum slip displacement reaches 10 cm and the residual one remains under 1 cm. In this case, the loose-soil segments at both sides of the main core are forced to move up and down with some internal deformation, supplying the system with restoring force. No distress is noted in the soil and thus soil failure is unlikely.

5. COMPARATIVE STUDY AND CONCLUSIONS

Summarizing the results of all dynamic analyses, we conclude that the most effective in-ground isolation geometries are the cylindrical and the compound trapezoidal. They outperform all others in that they result in substantial reduction of acceleration on the surface, with only limited relative displacements (maximum and permanent), without causing any local soil failure zones.

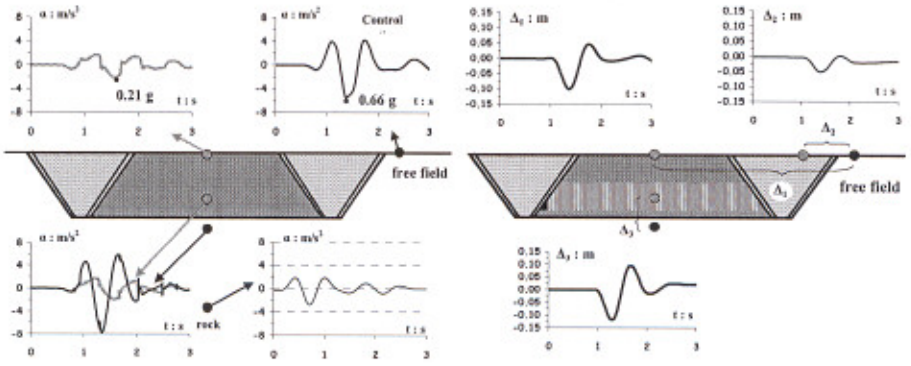

Figure 9 (a) Acceleration time histories, and (b) Relative displacement time histories for compound trapezoidal liner geometry. Control motion : Ricker $f_0 = 1$ Hz, $a_{ff,max} = 0.66$ g ; soft soil profile.

The results also show a clear reduction in transmitted acceleration for all the proposed geometries of the isolation liner, independently of soil profile. But the magnitude of transmitted acceleration, the developing slip displacements, and the soil deformation are all dependent mostly on the geometry of the soil–liner interface, and not directly on the properties of the isolated or the surrounding soil. Further research is needed to prove the "promising" beneficial effect of in-ground isolation to structures.

REFERENCES

Yegian M.K. & Kadakal U. (2004) Foundation Isolation for Seismic Protection Using a Smooth Synthetic Liner. *Journal of Geotechnical and Geoenviromental Engineering*, 1121-1130.

Yegian M.K. & Katan M. (2004) Soil Isolation for Seismic Protection Using a Smooth Synthetic Liner. *Journal of Geotechnical and Geoenviromental Engineering*, 1131–1139.

Fardis N., Georgarakos P., Anastasopoulos I., and Gazetas G. (2003) Sliding Isolation of Structures: Effect of Horizontal and Vertical Acceleration. *Proceedings of the FIB 2003 Symposium*, Athens , Greece, 474–475.

Constantinou M.C., Gazetas G. and Tadjbakhsh I. (1984) Stochastic Seismic Sliding of Rigid Mass Against Asymmetric Coulomb Friction. *Earthquake Engineering and Structural Dynamics*, 777-793.

Makris N. and Black C.J. (2004) Dimensional Analysis of Rigid-Plastic and Elastoplastic Structures under Pulse-Type Excitations. *Journal of Engineering Mechanics*, 1006–1018.

Skinner R.I., Robinson W.H., and McVerry G.H. (1993) *An Introduction to Seismic Isolation*. John Wiley & Sons.

Farzad N. and Kelly J. (1999) *Design of Seismic Isolated Structures. From Theory to Practice*. John Wiley & Sons.

Yegian M.K. and Lahlaf A.M. (1992) Dynamic Interfaces Shear Properties of Geomembranes and Geotextiles. *Journal of Geotechnical Engineering, ASCE*, 118(5):760–779.

Esterhuizen J.B., Filz G.M., and Duncan J.M. (2001) Constitutive Behavior of Geosynthetic Interfaces. *Journal of Geotechnical and Geoenviromental Engineering*, 834–840.

Jangid R. S. & Kelly J.M. (2001) Base isolation for near fault motions. *Earthquake Engineering & Structural Dynamics*, 691–707.